

# Modified citrate gel routes to ZnO-based varistors

Anne Lorenz, Jürgen Ott<sup>1</sup>, Martin Harrer<sup>1</sup>, Egon A. Preissner<sup>1</sup>,  
Adam H. Whitehead<sup>\*,1</sup>, Martha Schreiber<sup>1</sup>

*Christian Doppler Laboratory for Hybrid Materials, Austrian Research Centers Seibersdorf, A-2444 Seibersdorf, Austria*

Received 4 September 2000; received in revised form 23 October 2000; accepted 30 October 2000

---

## Abstract

Chemical routes, based on a modified citrate gel synthesis, were developed for the production of ZnO-based varistor powders and compared with the conventional mixed-oxide route. Green bodies of powders prepared by the chemical routes were found to undergo densification in one or two discrete steps (at 770 and 910°C) compared to multiple-step densification of the conventional powder. In addition, it was found that the microstructures and electrical properties of the sintered pellets, although of nominally similar chemical composition, varied according to the synthesis procedure. Pellets from the chemical routes showed smaller grain sizes, higher densities, more evenly distributed intergranular phases and higher non-linearity coefficients than those from the conventional mixed-oxide route. © 2001 Elsevier Science Ltd. All rights reserved.

**Keywords:** Citrate-gel process; Electrical properties; Microstructure-final; Varistors; ZnO

---

## 1. Introduction

From a technical standpoint several electrical parameters are required of commercial varistors, including particular breakdown voltages, nonlinearity coefficients and energy handling capabilities.<sup>1</sup> In order to obtain the requisite values of these parameters much work has focused on subtle adjustments of the type and proportions of minor additives and of the sintering conditions. However, most commercial varistors are prepared by a mixed-oxide synthesis procedure, in which all of the components are mixed together as fine powders and then sintered.

The non-linear electrical properties of ZnO varistors are determined by grain boundary phenomena, whilst the low-current behaviour is a function of both the quality of the grain boundaries and the intergranular phases. The conductivity of the grains, which influences the varistor performance at high currents, is dependent on the granular chemical composition. The minor components added to commercial ZnO varistors have been

found to influence not just the grain conductivity but also the grain growth, intergranular phases and grain boundaries. In accordance with common usage, the minor components shall be referred to here as dopants (grain conductivity enhancers) and additives (grain boundary formers).

One perceived problem with the mixed-oxide route is that no differentiation is made in the method of incorporation of additives and dopants. In addition impurities due to abrasion from the milling equipment may render the situation more complex. Generally high sintering temperatures and long sintering times are required to improve homogeneity and obtain satisfactory varistor pellets. However, chemical synthesis may offer routes to more homogeneous green bodies, requiring shorter sintering times at lower temperatures.

Dosch et al.<sup>2</sup> describe a process for ZnO varistor powder synthesis in which a co-precipitation process from chlorides was used. An interesting feature of this approach is related to the sequence of precipitation of the various constituents. The strategy employed was to separate the manufacturing process into several steps and to use the constituents in the appropriate step based on their later functionality. In this respect, the dopants were co-precipitated with ZnO, since they were required within the grains to enhance the electrical conductivity. After a calcination step, additives were precipitated

---

\* Corresponding author. Tel.: +43-2682-704400; fax: +43-2682-7044010.

E-mail address: [office@fwg.at](mailto:office@fwg.at) (A.H. Whitehead).

<sup>1</sup> Current address: Funktionswerkstoffe F & E GmbH, Marktstrasse 3, A-7000 Eisenstadt, Austria.

onto the surface of the doped ZnO grains. The additives were mostly responsible for the intergranular Schottky barrier formation and were also required to provide the flux for the liquid-phase sintering process. Related precipitation procedures are described by Haile<sup>3</sup> and Westin<sup>4</sup>. In these cases pure ZnO was covered by a coating of dopant and additive oxides.

In this work the citrate gel process was combined with the strategies of co-precipitation employed by Dosch<sup>2</sup> and precipitation by Westin<sup>4</sup> to prepare ZnO-based varistors. However, the citrate-gel process commonly employed<sup>5,6</sup> was modified by using acetates instead of nitrates of the relevant metals (except for Bi and Al for which nitrates were used and Si for which the tetraethoxide was used). Acetates were preferred over nitrates as they produced less toxic side products during powder calcination.

## 2. Experimental

Varistors composed of the following were prepared: ZnO with Co, Mn, Al, Ni, and Cr dopants, and Bi, Sb, Ba, Si, and B additives. The total amount of dopants and additives equalled 7 at. %.

The conventional mixed-oxide route, used to prepare reference samples, is denoted as route 0. Powders prepared by this route were obtained from Siemens-Matsushita.

Route 1 synthesis involved a first step in which doped ZnO powder was prepared by coating a ZnO powder with a layer of citrates of the dopants using the citrate-gel technique. Explicitly, individual solutions of each precursor material were made by dissolving the relevant dopant metal salts (Co, Mn, Al, Ni, Cr) in aqueous citric acid solution. At least 2 mol equivalents of citric acid to each minor component were used. Citrate solutions of each dopant were added sequentially to a suspension of ZnO powder in de-ionised water.

The suspension was stirred with a sawtooth mixer for up to 18 h and then dehydrated at temperatures up to 70°C under reduced pressure until a dry powder was obtained. The powder was then dried overnight at 70°C prior to calcining at 480°C for 4 h.

In the second step the doped ZnO powder was coated with a layer of the additives. Citrate solutions of the additives were prepared in the following ways. The barium and boron salts were dissolved in citric acid with a minimum amount of water.  $\text{Si}(\text{OEt})_4$  was diluted in ethanol. Antimony acetate was added directly to the citric acid and stirred vigorously for about 30 min. The bismuth salt,  $\text{Bi}(\text{NO}_3)_3 \cdot 5\text{H}_2\text{O}$ , was added to a solution containing 10 mol equivalents of citric acid. A solution of 5 mol  $\text{dm}^{-3}$   $\text{NH}_4\text{OH}$  was added dropwise under vigorous stirring until a pH value of 7 was achieved, coinciding with complete dissolution of the salt.

The doped ZnO powder was added to a reaction vessel containing the bismuth salt solution, which was stirred continuously. Subsequently, the citrate solutions of the other additives were transferred sequentially to the reaction vessel and the resulting suspension stirred for about 18 h. The solvent was removed completely in a rotary evaporator under reduced pressure to yield a solid material that was then calcined under an ambient atmosphere at 480°C for 4 h. This second calcination step led to doped ZnO powders which were coated with a layer of additive oxides.

For route 2, as for route 1, a doped ZnO powder was produced initially. The doped powder was prepared by co-precipitation of zinc citrate and citrates of the dopants from an aqueous solution.

Individual citrate solutions of the dopants, as described above for route 1, were added to the clear, colourless zinc-citrate solution. After stirring for about 30 min the solution was dehydrated in a rotary evaporator under reduced pressure to produce a highly viscous gel. Crystallisation of the gel occurred by ageing for 16 h at room temperature or slightly above. The citrate powder was then calcined in air at 480°C for 4 h to remove the organic components.

The second step of route 2, to coat the doped ZnO powder with a layer of additives, was identical to that described for route 1 above.

The powders from routes 0, 1 and 2 were individually ground with a pestle and mortar. Each powder was then granulated with the addition of an organic binder mixture (2%, obtained from Siemens-Matsushita). The granules were dried and sieved prior to palletising. Four hundred milligrams of a given powder was uniaxial pressed to form each 10 mm diameter pellet.

After thermal removal of the binder at 400°C green bodies were formed. Using a dilatometer, measurements of the normalised change in sample thickness (linear expansion,  $\Delta L/L_0$ ) were made with increasing temperature (heating rate 3°C min<sup>-1</sup> in air) on green bodies prepared by the three routes. The differential length change with temperature (differential linear expansion,  $d(\Delta L)/dT$ ) was also calculated.

Sintered pellets were prepared from the green bodies by heating in air to 1000°C for 90 min (heating rate 3°C min<sup>-1</sup>, cooling rate 1°C min<sup>-1</sup>) which yielded dark grey ceramic bodies of approximately 1.2 mm thickness.

The distribution of the intergranular phase of each sintered and polished specimen was observed by scanning electron microscopy (SEM, Zeiss DSM 950). Grain size measurements were made on samples that had been thermal etched after polishing.

In order to make electrical measurements varistor samples were polished and contacted on both opposing faces with fired-on silver paste received from Siemens-Matsushita. The geometric area of each contact was 20 mm<sup>2</sup>. Several samples (2–7) were prepared for each

route and the reported values represent an average of these measurements.

The nonlinear coefficients  $\alpha$  were evaluated by the relationship given in Eq. (1).

$$\alpha = \frac{\log I_2 - \log I_1}{\log V_2 - \log V_1} \quad (1)$$

where  $V_1$  and  $V_2$  are the voltages corresponding to the currents  $I_1$  and  $I_2$  respectively. The nonlinearity coefficient,  $\alpha_1$  was calculated  $I_1 = 10 \mu\text{A}$  and  $I_2 = 1 \text{ mA}$ .  $\alpha_2$  was calculated when  $I_1 = 1 \text{ mA}$  and  $I_2 = 10 \text{ A}$ .

ZnO-based varistors are often characterised by a breakdown field strength that marks the transition from the linear pre-breakdown region to the non-linear region. We have chosen to measure the breakdown field strength ( $E_V$ ) at a current of 1 mA. From  $E_V$  and the SEM measurements of grain size the average voltage per grain boundary  $V_{gb}$  was calculated.

### 3. Results and discussion

As shown in Figs. 1–3, by the differential linear expansion with temperature, the green bodies from

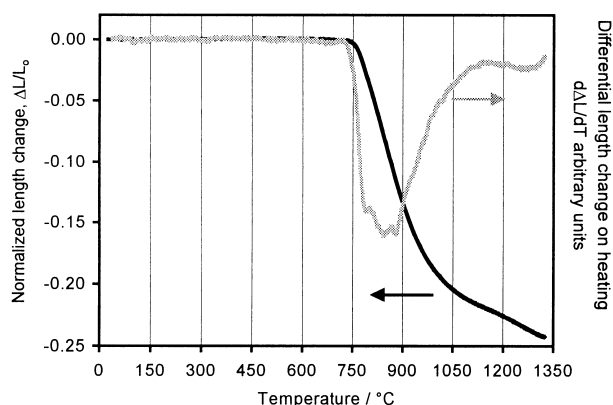


Fig. 1. Dilatometer curve (heating rate  $3^\circ\text{C min}^{-1}$ ) for a route 0 sample.

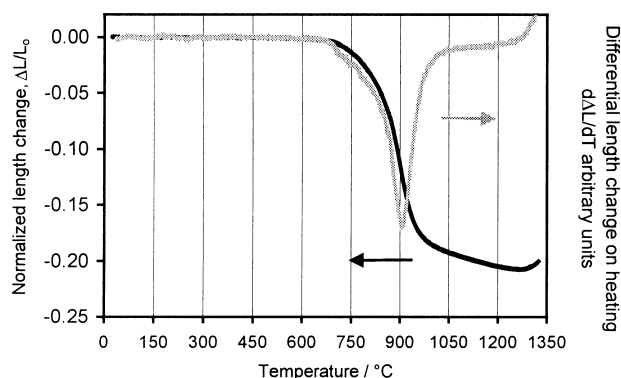


Fig. 2. Dilatometer curve (heating rate  $3^\circ\text{C min}^{-1}$ ) for a route 1 sample.

route 1 showed a slightly earlier onset of densification than for routes 0 and 2 ( $680^\circ$  compared with  $730$ – $750^\circ\text{C}$ , respectively). However, more strikingly the densification of materials from routes 1 and 2 was largely complete (the magnitude of  $\Delta L/L_0$  was 95% of the maximum value) at  $1100$  and  $980^\circ$  respectively, compared with  $>1200^\circ\text{C}$  for the route 0 material.

Local maxima were observed close to  $770^\circ\text{C}$  for the green bodies from routes 0 and 2 (Figs. 1 and 3, respectively) which may be attributed to the formation of a bismuth-rich liquid,<sup>7</sup> whereas the route 1 green body showed only a single local maxima at  $910^\circ\text{C}$  (Fig. 2).

The formation of an extensive liquid phase in the route 1 material at  $770^\circ\text{C}$  was presumably inhibited by the minor components. Because the route 1 and 2 green bodies densified at different temperatures it may be reasoned that the two strategies produced green bodies which differed in their local distributions of minor components. The most obvious and probable difference would have arisen from the incomplete diffusion of the dopants (Co, Mn, Al, Ni, Cr) into the ZnO grains under route 1.

The low surface concentration of dopants and high surface concentration of additives under route 2, and in localised regions of the green bodies under route 0, was suitable for the formation of a liquid phase at  $\sim 770^\circ\text{C}$ . A further densification process at  $\sim 910^\circ\text{C}$  was common to pellets from all three routes and may have involved the formation of a liquid phase containing both additives and dopants. Hence the route 1 powder would have densified primarily through the formation of a single liquid phase, whereas the route 2 powder underwent a two-stage densification. Densification of the route 0 powder proceeded through a number of steps (at least three) reflecting the large variations in the local dopant and additive concentrations arising from the precursor powders.

From Table 1 the green bodies of samples derived by routes 1 and 2 had lower densities than those from the conventional route 0. After sintering, the densities of all

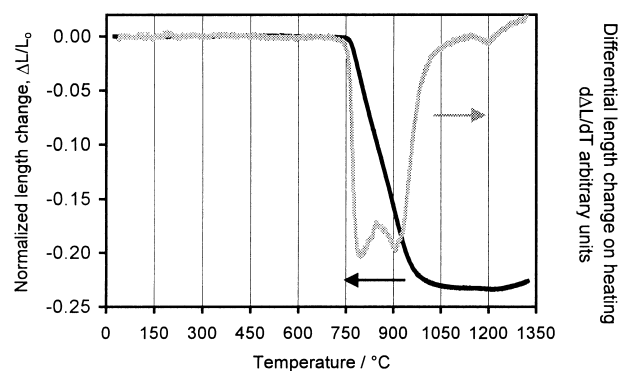


Fig. 3. Dilatometer curve (heating rate  $3^\circ\text{C min}^{-1}$ ) for a route 2 sample.

Table 1  
Comparison of green and final density for the three synthetic routes

Synthesis route	Green density (% theoretical maximum)	Sinter density (% theoretical maximum)	Average grain size ( $\mu\text{m}$ )
0	$58.0 \pm 0.9$	$94.8 \pm 1.3$	$7.4 \pm 0.7$
1	$55.0 \pm 0.9$	$95.7 \pm 1.3$	$5.9 \pm 0.5$
2	$49.1 \pm 0.8$	$97.1 \pm 1.1$	$5.6 \pm 0.5$

three types of pellets increased. The sintered body densities increased in the order route 0 < route 1 < route 2, as may have been expected from the more rapid densification of the novel materials.

SEM examination of the routes 1 and 2 samples showed similar homogeneous distributions of the intergranular phases and ZnO grains. This contrasted with the route 0 sample, which showed a distinctly inhomogeneous distribution. In particular aggregates of intergranular material of  $\sim 4 \mu\text{m}$  diameter were clearly visible. Thus, some of the inhomogeneity of the starting materials was retained, even after sintering at  $1000^\circ\text{C}$ .

The average grain sizes (Table 1) were similar for the two chemical routes ( $5.6$  and  $5.9 \mu\text{m}$ ) and significantly less than the route 0 sample. A more homogeneous distribution of spinel phases, which inhibit grain growth,<sup>8</sup> in both the routes 1 and 2 pellets as compared with those from route 0, may explain the larger grain size of the conventional material.

The values of the characteristic field strengths and non-linear coefficients are listed in Table 2. From which it may be noted that the  $\alpha_1$  and  $E_V$  values for the samples prepared by routes 1 and 2 are higher than those previously reported from the citrate gel route<sup>6</sup> ( $E_V = 443 \text{ V mm}^{-1}$ ,  $\alpha = 27.8$ ), possibly due to the lower sintering temperatures employed in this work ( $1000^\circ\text{C}$  as compared with  $1200^\circ\text{C}$ ). Also the values of  $\alpha_1$  are similar for the route 1 and 2 samples and significantly higher than those of the route 0 material. This would imply that more homogeneous interfaces were produced by the modified citrate-gel routes. However, it should be noted that the values of  $V_{\text{gb}}$  were within experimental error of one another and close to those reported previously.<sup>9</sup>

The values of  $\alpha_2$  (Table 2) may be taken to indicate that the high-current behaviours of the pellets produced by the three routes were similar.

Table 2  
Characteristic field strength, grain boundary voltage and non-linear coefficients of sintered samples prepared by routes 0, 1 and 2

Synthetic method	$E_V$ ( $\text{V mm}^{-1}$ )	$V_{\text{gb}}$ (V)	$\alpha_1$	$\alpha_2$
Route 0	$380 \pm 20$	$2.8 \pm 0.3$	$47 \pm 4$	$34 \pm 3$
Route 1	$460 \pm 30$	$2.7 \pm 0.3$	$72 \pm 9$	$35 \pm 3$
Route 2	$510 \pm 30$	$2.9 \pm 0.3$	$75 \pm 15$	$34 \pm 3$

#### 4. Conclusions

Dense, doped ZnO ceramic pellets were produced by three different synthetic methods; conventional mixed-oxide, precipitation and co-precipitation citrate gel. The two non-conventional routes produced precursor powders which sintered more readily and in fewer distinct stages (one or two compared with many) than a powder prepared by the conventional mixed-oxide route. This was attributed to the tailored microstructural variations in minor component concentrations for the novel routes compared with the random, inhomogeneous nature of the conventional, mixed-oxide material.

ZnO-based varistors prepared by a modified citrate gel route showed higher values of characteristic field strengths and non-linear coefficients ( $\alpha_1 \sim 70$ ) when compared with varistor ceramics produced by the mixed-oxide route ( $\alpha_1 = 47$ ). However, the values of  $V_{\text{gb}}$  and  $\alpha_2$  were similar. Because the citrate-gel routes led to smaller grain sizes (and  $V_{\text{gb}}$  was relatively constant) the breakdown field strengths were higher than samples prepared by the mixed-oxide route.

#### Acknowledgements

We thank Siemens-Matsushita, Deutschlandsberg (now EPCOS) for providing materials. Discussions with Professor J. Schoonman are gratefully acknowledged.

#### References

- Gupta, T. K., Application of zinc oxide varistors. *J. Am. Ceram. Soc.*, 1990, **73**, 1817–1840.
- Dosch, R. G., Tuttle, B. A. and Brooks, R. A., Chemical preparation and properties of high-field zinc oxide varistors. *J. Mater. Res.*, 1986, **1**, 90–99.
- Haile, S. M., Johnson, J. D. W., Wiseman, G. H. and Bowen, H. K., Aqueous precipitation of spherical zinc oxide powders in varistor application. *J. Am. Ceram. Soc.*, 1989, **72**, 2004–2008.
- Westin, G., Ekstrand, A., Nygren, M., Österlund, R. and Merkelbach, P., Preparation of ZnO-based varistors by the sol-gel technique. *J. Mater. Chem.*, 1994, **4**, 615–621.
- Marilly, C., Courty, P. and Delmon, B., Preparation of highly dispersed mixed oxides and oxide solid solutions by pyrolysis of amorphous organic precursors. *J. Am. Ceram. Soc.*, 1970, **53**, 56–57.
- Fan, J. and Sale, F. R., Citrate gel route processing of zno

- varistors. In *Electroceramics: Production, Properties and Microstructures*, ed W. E. Lee and A. Bell. Ashgate Publishing Company, London, 1994, pp. 151.
7. Leite, E. R., Nobre, M. A. L., Longo, E. and Varela, J. A., Microstructural development of ZnO varistor during reactive liquid phase sintering. *J. Mater. Sci.*, 1996, **31**, 5391–5398.
  8. Wong, J., Rao, P. and Koch, E. F., Nature of an intergranular thin-film phase in a highly non-Ohmic metal oxide varistor. *J. Appl. Phys.*, 1975, **46**, 1827–1830.
  9. Olsson, E. and Dunlop, G. L., Characterization of individual interfacial barriers in a ZnO varistor material. *J. Appl. Phys.*, 1989, **66**, 3666–3675.